

STUDY ON THE INFLUENCE OF PROCESS PARAMETERS ON SURFACE PROPERTIES OF ADDITIVELY MANUFACTURED PARTS

Sara Varetti^{1*}, Marco Boccaccio², Valentina Trimini^{1,3}, Ignazio Scavo⁴, Francesco Flora⁵
Francesco Acerra⁶ and Stefano Corvaglia⁴

¹ Leonardo Spa, Leonardo Labs - Materials, Grottaglie, Italy,

² Leonardo Spa, Leonardo Labs - Materials, Torino, Italy,

³ Politecnico di Bari, Faculty of Mechanics, Mathematics and Management Engineering, Bari, Italy,

⁴ Leonardo Spa, Aerostructures Division, Grottaglie, Italy,

⁵ Leonardo Spa, Leonardo Labs - Materials, Pomigliano, Italy,

⁶ Leonardo Spa, Aircrafts Division, Pomigliano, Italy.

* Corresponding author (sara.varetti.ext@leonardo.com)

Keywords: *Additive Manufacturing, Carbon PEEK, mechanical testing.*

ABSTRACT

Additive Manufacturing (AM) of high performance techno-polymers like ULTEM and PEEK is gaining an increasing interest in various industrial sectors. Fusion Deposition Modeling (FDM), one of the most popular AM techniques, offers exciting opportunities in the printing of high quality thermoplastic polymer composites. The performances of parts produced in FDM are influenced by many process parameters, such as material deposition speed, printing strategy, layer thickness, nozzle and chamber temperature. The present work focuses on the use of different machines and batches of material and studies their influence on the mechanical tensile performance of the printed samples. Roughness of specimens is analysed to correlate the mechanical performances to the surface features. The specimens were produced using a Roboze Argo 500 machine: the nozzle and chamber temperature were fixed at 450°C and 180°C respectively, layer thickness at 0.225mm, nozzle diameter at 0.4mm and 100% infill were used for all specimens. Scanning electron microscopy was used to study the quality and orientation of the printed samples.

1 INTRODUCTION

Additive Manufacturing (AM) 3D Printing technologies are processes of growing interest in several fields, including aerospace, both in metals and polymers. These manufacturing technologies offer several advantages, such as an *in-situ* production of parts, the ability to make complex structures especially if the design is the result of topological optimization, and the reduction of waste by depositing material only where it is needed [1]. In the field of polymers, particular attention is paid to the production of parts made of techno-polymers such as PEEK (poly-ether-ether-ketone), PEI (poly-ether-imide), PEKK (poly-ether-ketone-ketone) and Nylon [2]. These are thermoplastic polymers with high mechanical strength, even at high temperatures, and good chemical resistance. They are either used in the pure version or combined with short reinforcing fibres, most often Carbon fibres [3]. Furthermore, several currently available 3D printing machines can extrude thermoplastic polymer matrix reinforced by continuous carbon fibres [4]. The most widely used additive technology for printing thermoplastic polymers is Fusion Deposition Modeling (FDM) or Fused Filament Fabrication (FFF). With FDM technology, parts are made layer by layer by the movement of a deposition head, which extrudes the filament of the material used in the areas indicated by the 3D model [5]. Before printing, the 3D model can be processed with different softwares, namely Cura, Slicer or Simplify 3D, thus allowing careful selection of process parameters, and generates a file including all the information needed for the production process (i.e. .gcode file) [6]. For printing techno-polymers, AM machines with special features are used, such as the building chamber heated up to high temperatures and nozzles suitable for high printing temperatures and to resist damage due to carbon fibres in the filament [7]. Printed

components are near-net-shape and require only a few finishes before they can be used, such as the removal of supports and any additional heat or surface treatments.

3D printing allows to vary a large number of process parameters, such as print speed, infill percentage, layer thickness, extrusion temperature, print chamber temperature and others. For the same material, each of these parameters affects, to different degrees, the final properties of the part [8-9]. To use this technology for full scale component manufacturing, it is necessary to control the quality and the properties of components, using simple and repeatable methods.

In the study presented in this paper, surface roughness was chosen as control parameter of the parts. Based on the machine knowledge, this value varies according to the process parameters chosen and is indicative of quality of the printing and of possible problems during manufacturing. This method would allow an early evaluation of the process parameters variation and its influence on the printed parts, thus providing good potential for optimization of the process parameters of the machine and for tuning them with the desired material properties.

2 MATERIALS AND METHODS

For this study, Carbon PEEK specimens were produced using the Roboze Argo500 3D printer (Table 1) and the commercial material Ketaspire® CF10 LS1 AM Filament. The filament is made by PEEK matrix reinforced with 10% of short carbon fibers; main properties are listed in Table 2.

Feature	Value
Working volume [mm ³]	(X)500 x (Y)500 x (Z)500
Chamber temperature [°C]	180
Extruder temperature [°C]	450
Extruder diameter [mm]	0.4
Layer thickness [mm]	0.225

Table 1: Roboze Argo500 features [10].

Property	Solvay datasheet [11]	Roboze datasheet [12]
Filament Diameter [mm]	1.75	1.75
Density [g/cm ³]	1.33	1.33
Tensile Strength at Break [MPa]	140	136
Tensile Modulus [GPa]	11.0	9.1
Tensile Elongation at Break [%]	1.7	2.2

Table 2: Ketaspire® CF10 LS1 datasheet – properties at 0° strategy.

Instead of the traditional printing plate present in all FDM machines, the Argo500 has a surface connected with a vacuum system, which holds a PEI-based thermal layer. The thermal layer allows adequate adhesion of the C-PEEK to the work surface (the material does not easily adhere to the surfaces present in traditional FDM machines due to the high shrinkage of PEEK). At the end of the printing process, the vacuum is turned off and the thermal layer can be released with the C-PEEK parts attached. Supports and rafts are inserted between the parts and the thermal layer, which allow to remove the thermal layer without damaging the C-PEEK parts and reduce the deformation of the components due to the cooling shrinkage.

All specimens were printed with an infill rate of 100% and a printing strategy of 0°, using two different Argo500 printers and three different batches of filament. Each printer and batch combination has been identified by a different Case, as shown in Table 3.

The roughness of the specimens is measured by a roughness meter, the porosity is evaluated by specimen weight and Optical Microscope (model Hirox RH – 2000) analysis of the cross section. The specimens were produced flat on the building plate and the supports, as shown in Figure 1, and removed

by CNC machining. ASTM D3039 [13] was used for specimen preparation and tensile testing (Figure 2) and the nominal dimensions of the samples are 4.05mm x 25.4mm x 254mm. The tabs used are Aluminium alloy (EN AW 6082) and were attached to the specimens through a two-component epoxy glue (Araldite 2031-1 Huntsman).



Figure 1: Printed specimens as-built before CNC machining.

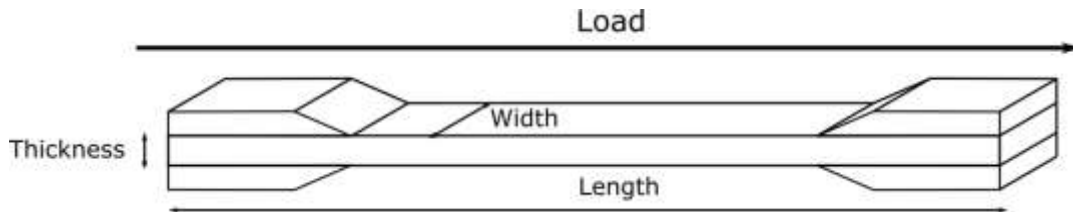


Figure 2: Standard specimens for tensile tests according to ASTM D3039 [13].

Case 1	Case 2	Case 3	Case 4	Case 5	Case 6
Printer 1	Printer 1	Printer 1	Printer 2	Printer 2	Printer 2
Batch 1	Batch 2	Batch 3	Batch 1	Batch 2	Batch 3

Table 3: Cases features.

According to ASTM D3039 [13], all specimens were subjected to tensile test with constant axial speed of 2 mm/min. The ultimate strength was calculated for all the specimens as maximum load on nominal cross section. The modulus was calculated in two different ways depending on the Case: by extensometer for Case 1, 3, 4, 5 and 6, by two-way Strain Gage (SG) for Case 2. It was originally planned to use the two-way Strain Gage for all Cases with the goal of detecting both modulus and Poisson ratio. Due to the large number of specimens, it was not possible to use the Strain Gage for all of them, and it was decided to choose a reference Case (Case 2) to evaluate how the Poisson ratio varies as the printing strategy changes. For all other specimens, an unidirectional extensometer was used to calculate the modulus only. An MTS machine (model 370.25 Landmark Load Frame) with a load cell of 250 kN was used for Cases 1, 3, 4, 5, 6 and an INSTRON machine (model 5582) for Case 2. The final tensile specimens and the tensile test setup are shown in Figure 3. The specimens were also analysed by a digital Optical Microscope Hirox RH – 2000, after cutting and polishing, and fracture surfaces were observed by SEM Zeiss.

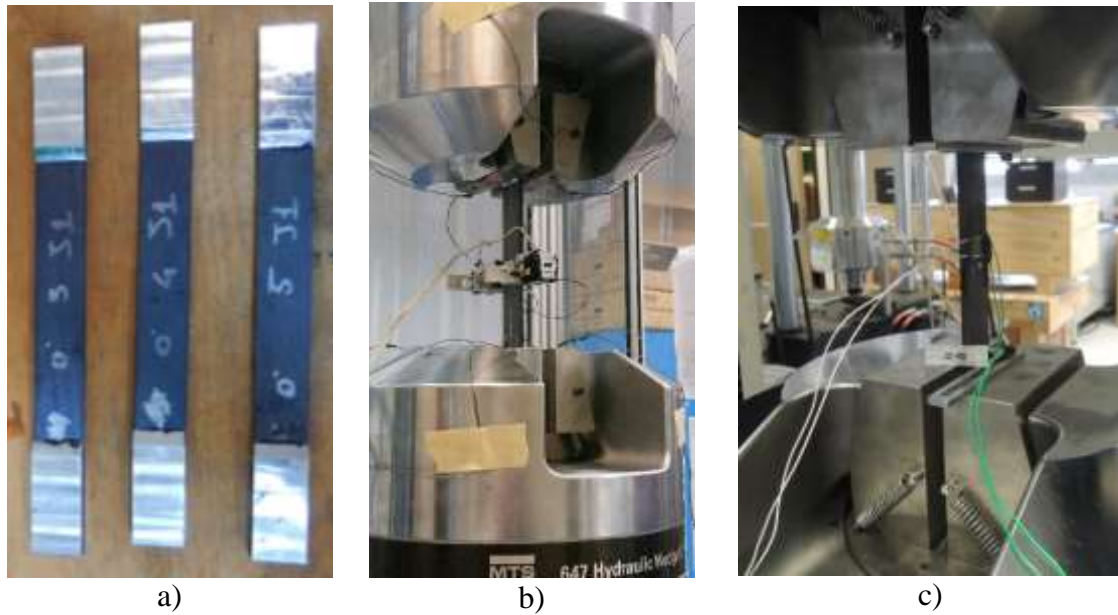


Figure 3: a) Tensile specimens, b) MTS machine setup with extensometer and c) Instron machine setup with Strain Gage (used for Case 2).

3 RESULTS AND DISCUSSION

3.1 Mechanical characterisation

The Ultimate Strength and Elastic Modulus for all the Cases for the specimens printed with a 0° strategy, are shown in Table 4 and Figure 4. The good performances of 0° samples can be explained by the fact that the direction of filament deposition coincides with the direction of load application and the welding between the filaments within the same layer and between one layer and another is good. For Case 1, both Ultimate Strength and modulus present good values and low standard deviation. The 0° specimens, after a plastic deformation, failed mainly along 45° with respect to the load direction (as shown in Figure 5) and the break propagates longitudinally to the length of the sample. The mechanical performance and the observed dispersion of the data in Case 2 specimens is consistent with that seen for Case 1, but it should be mentioned that this Case testing was performed using different instrumentation (SG for the modulus and INSTRON as test machine). Also the fracture mechanism is similar to what seen in the other cases. After a plastic deformation, failed mainly along 45° with respect to the load direction, but the break occurs without propagation longitudinally in the sample (Fig. 5). For Case 3, as presented in Figure 5, failure is similar to Case 1. The standard deviation is low and the data is consistent with the previous cases. The results of mechanical test on 0° specimens for Case 4 present some differences: they have much lower modulus and Ultimate Strength values. The average E modulus is 7630 MPa and the average Ultimate Strength is 111 MPa, which are much lower when compared for example with Case 3 with an E modulus of 9290 MPa and Ultimate Strength of 156 MPa. To better understand the behaviour of these specimens, Optical Microscope cross-section images are shown in Figure 6b. Figure 6b is representative of all the 0° specimens in Case 4, and the cross-section can be compared with that of Case 3 (Fig. 6a). Figure 6a depicts the cross-section of a 0° specimen, obtained by cutting the sample along the plane perpendicular to the filament deposition. The image is representative of the cross-section of all the 0° specimens for all the cases, except for Case 4. In the image, the shape of the deposited filament can be distinguished and the presence of evenly distributed pores in the section can be seen. Furthermore, the specimens in Case 4 have a larger amount of pores and these are distributed unevenly in the cross-section. In some points, the pores are very enlarged and prevent adhesion between the layers and overall reduce the effective resistant section of the specimens, lowering the mechanical performance. In addition, all the specimens have much higher surface

roughness than the other cases. Observing the high amount of large pores in the upper right part of the section, it was hypothesized that the phenomenon may be due to the uneven deposition of material by the nozzle and the consequent release of lumps that are dragged by the nozzle, forming grooves in the specimen during the deposition of new material. The cause could be a lowering of the extrusion temperature, which would make the PEEK less fluid and more prone to the formation of lumps. To verify this aspect, it would be necessary to monitor the extrusion temperature during the process. Alternatively, it can be assumed that there were longer or more aggregated carbon fibres in a section of filament that caused the nozzle obstruction. For Case 5 and Case 6 the standard deviation is low and the data is consistent with the previous cases. The only anomaly is one 0° specimen of Case 5 that has an Ultimate Strength of 131 MPa, lower than the average of the others in its group that break at 154 MPa. This specimen has the same cross-section as the 0° specimens in Case 4 and the same high surface roughness. The hypothesis is that, in this sample, there was nozzle clogging and the lumps released and carried around by the deposition head that created the grooves.

From Table 5 it can be seen that the best results in terms of Ultimate Strength and E modulus are for the first three cases, which share the Printer 1. The specimens in Case 4 and one specimen in Case 5 have defects that cause the mechanical properties to be lowered. The modulus of Case 2 is higher than the others, but the reason may be the measurement by SG.

Property	Case 1	Case 2	Case 3	Case 4	Case 5	Case 6
Ultimate Strength [MPa]	153	155	154	111	149	150
StD. UTS [%]	2.0	4.3	2.3	4.2	6.9	4.8
E modulus [MPa]	8858	10589	9154	7630	8322	8671
StD. E [%]	1.6	5.7	7.2	2.2	6.2	4.4

Table 4: Tensile test results for 0° of all cases.

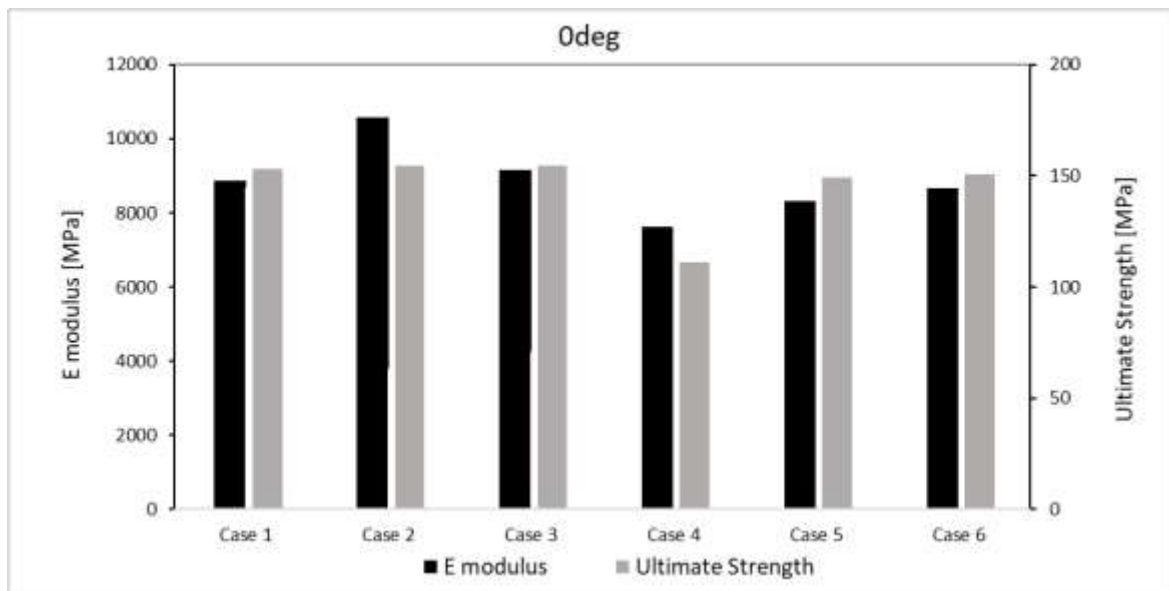


Figure 4: Results of tensile tests on 0° specimens for all cases in terms of Ultimate Strength and E modulus.

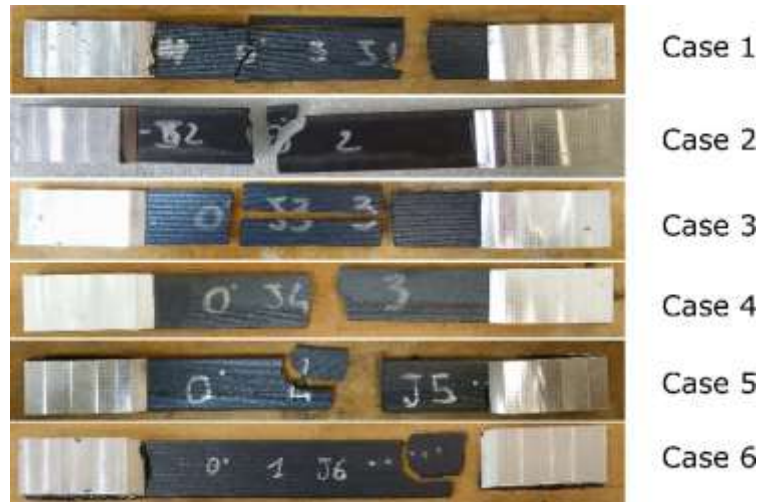


Figure 5: Photos of 0° specimens after failure for different cases.

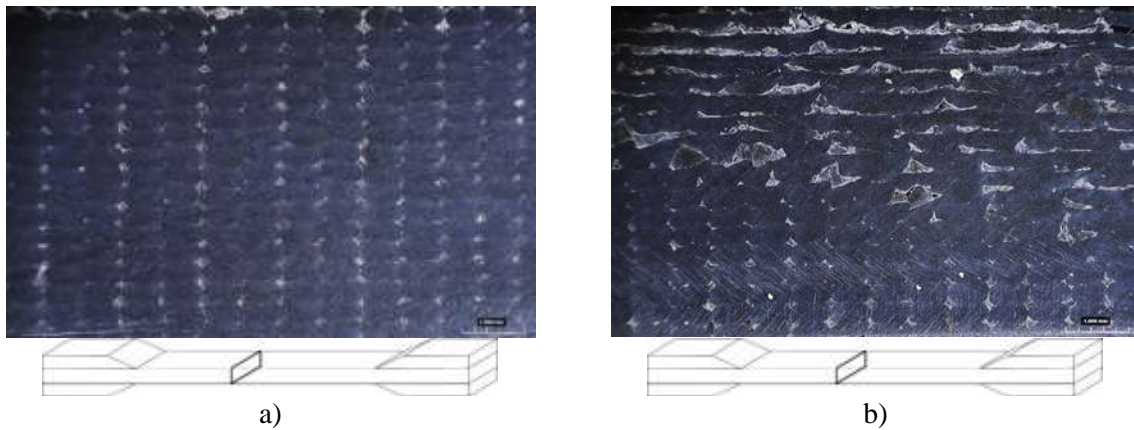


Figure 6: Cross-section 0° specimens: a) Case 3 sample n.4 (158 MPa) and b) Case 4 sample n.2 (105 MPa).

3.2 Roughness evaluation

In Table 5 the values of roughness of all the specimens tested are reported. It is possible to note that higher is the roughness measured, lower are the mechanical performances. This aspect is also highlighted in Figure 7, which provides a detailed comparison between the roughness measured along the two direction and the ultimate strength (Figure 7). With these regards, it can be noted that for the majority of the measurements, a higher roughness along 0° has been depicted for Batch 1 and Batch 2, in which the values also tend to converge in both directions (i.e. roughness and ultimate strength) as the batch varies, up to the point where the average values are mostly equivalent (Batch 3).

Case 4 specimens, which exhibited lower mechanical properties than the other Cases and higher porosity, show higher roughness along both 0° and 90°. The same thing can be observed for specimen number 4 of Case 5.

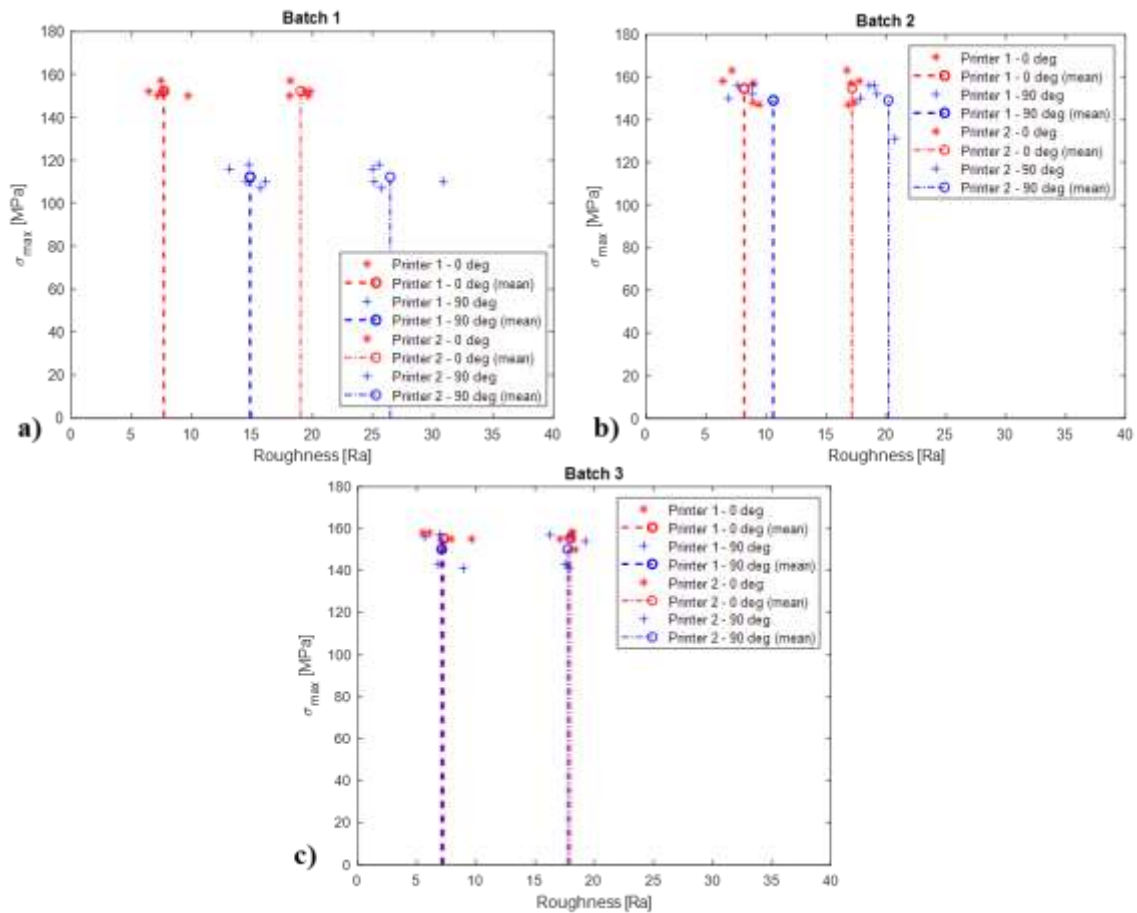


Figure 6: Comparison between the roughness measured along the two direction and the ultimate strength: a) Batch 1; b) Batch 2; c) Batch 3.

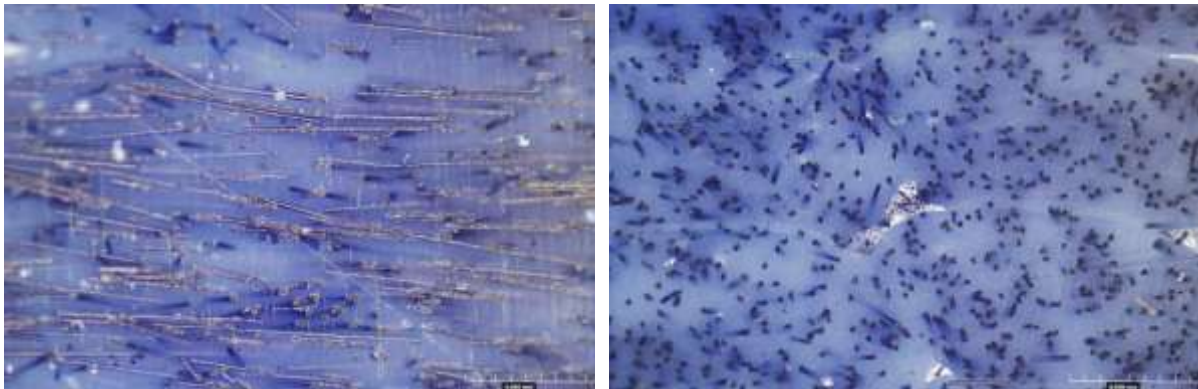
Specimen ID	Roughness along 0°[Ra] - average	Roughness along 90°[Ra] - average	E [GPa]	σ_{max} [MPa]
Case 1_1	7.19	19.65	8887	150
Case 1_2	7.66	19.38	8679	152
Case 1_3	6.45	19.82	8966	152
Case 1_4	7.46	18.18	9007	157
Case 1_5	9.71	18.13	8751	150
Case 2_1	8.93	17.41	10163	148
Case 2_2	9.45	16.86	9877	147
Case 2_3	6.41	17.78	10492	158
Case 2_4	7.16	16.76	11169	163
Case 2_5	8.96	17.09	11247	157
Case 3_1	7.91	18.16	8980	155
Case 3_2	7.17	18.38	8616	150
Case 3_3	5.50	18.09	8887	158
Case 3_4	6.06	18.18	8995	158
Case 3_5	9.63	17.10	10296	155
Case 4_1	16.12	38.86	7517	110
Case 4_2	15.69	25.72	7400	107
Case 4_3	14.54	25.14	7766	110
Case 4_4	14.74	25.54	7695	118

Case 4_5	13.15	25.02	7772	116
Case 5_1	8.86	19.26	8463	152
Case 5_2	7.63	19.04	8747	156
Case 5_3	8.91	18.61	8632	156
Case 5_4	20.76	26.25	7441	131
Case 5_5	6.88	17.89	8327	150
Case 6_1	5.68	17.77	8909	156
Case 6_2	7.11	19.24	8670	154
Case 6_3	8.92	17.87	8048	141
Case 6_4	6.82	17.55	8690	143
Case 6_5	6.95	16.24	9036	157

Table 5: Roughness and mechanical performances of all specimens tested.

3.3 Fibres orientation

The contribution of Carbon fibres within the PEEK matrix was evaluated through observations of the sections by OM and SEM. From Figure 8 obtained in the OM, the orientation of the Carbon fibres within the specimen can be observed: they are all strongly oriented in the direction of extrusion of the filament. This is initially due to the filament extrusion and subsequently to the second extrusion of the already formed filament to print the piece. This type of orientation contributes a lot to increasing the mechanical properties of the 0° specimens compared to the same specimens produced with the matrix alone, while it does not provide many benefits to the 90° specimens, as the fibres do not contribute to reinforce the adhesion between the filaments. Figure 9 depicts two SEM images of the fracture surface of a specimen at 0° . Also in this case there is a strong orientation of the fibres in the direction of extrusion, the adhesion of matrix and fibres is good, but in many places there are holes where fibre pull out occurred. The contact between the Carbon fibre and the PEEK matrix is difficult due to the high shrinkage of the matrix at cooling, which causes a detachment. A surface treatment of the fibres and an increase in the extrusion temperature could improve adhesion and therefore also the mechanical properties [14].

Figure 8: OM images of fibers in 90° specimens in the a) longitudinal section and b) perpendicular section with respect to the direction of filament deposition.

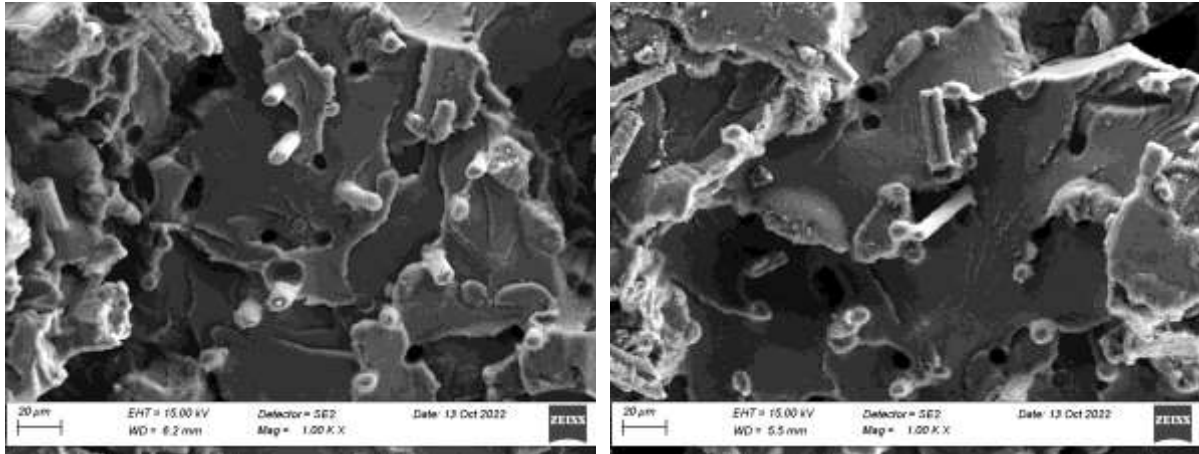


Figure 9: SEM image of a failure surface of a 0° printed specimen.

5 CONCLUSIONS

From this preliminary characterisation of the Carbon PEEK Ketaspire® CF10 printed with the Roboze Argo500 machine, it was possible to compare two different parameters: the machine and the batch of material. The specimens were printed in six different Cases by varying three batches of material and two machines of the same type, to observe the influence of these factors on mechanical tests. The greatest influence is given by the machine used: it seems that the specimens produced with Printer 1 (Cases 1, 2 and 3) have less dispersed and more repeatable results than those of the specimens obtained with Printer 2 (Cases 4, 5 and 6). This aspect has been confirmed by the comparison between the roughness measured in the two direction and the mechanical properties. Indeed, the majority of the specimens printed at 0° showed lower Ultimate Strength than average value due to an anomalous presence of pores inside, which greatly reduced the resistant section. This results can be traced back to differences in the extrusion temperature and more generally to the machine hardware. Better process control would be required to ensure repeatability of results on all machines. Among the developments foreseen in the future there is the improvement of the hardware through sensors and a project for monitoring the process parameters that allows to identify the trend of the variables and correlate them to the results obtained from the specimens.

REFERENCES

- [1] J. M. Jafferson and D. Chatterjee “A review on polymeric materials in additive manufacturing”. *Mater. Today: Proc.*, Vol. 46, pp 1349–1365, 2021.
- [2] A. E. Magri, S. Vanaei and S. Vaudreuil “An overview on the influence of process parameters through the characteristic of 3D-printed PEEK and PEI parts”. *High Perform. Polym.*, Vol. 33, No. 8, pp 1–19, 2021.
- [3] P. Wang, B. Zou, S. Ding, et al. “Effects of FDM-3D printing parameters on mechanical properties and microstructure of CF/PEEK and GF/PEEK”. *Chinese J. Aeronaut.*, Vol. 34, No. 9, pp 236-246, 2020.
- [4] B. Chang, X. Li X, P. Parandoush, et al. “Additive manufacturing of continuous carbon fiber reinforced poly-ether-ether-ketone with ultrahigh mechanical properties”. *Polym. Test*, Vol. 88, 106563, 2020.
- [5] S. Berretta, R. Davies, Y. T. Shyng, et al. “Fused Deposition Modelling of high temperature polymers: Exploring CNT PEEK composites”. *Polym. Test.*, Vol. 63, pp 251-262, 2017.
- [6] Duong, T. H., Jaksic, N. I., DePalma, J. L., Ansaf, B., Daniel, D. M., Armijo, J., & Galaviz, M. (2018). G-code visualization and editing program for inexpensive metal 3D printing. *Procedia Manufacturing*, 17, 22-28.
- [7] Heidari-Rarani, M., Rafiee-Afarani, M., & Zahedi, A. M. (2019). Mechanical characterization of FDM 3D printing of continuous carbon fiber reinforced PLA composites. *Composites Part B: Engineering*, 175, 107147.
- [8] Yang, C., Tian, X., Li, D., Cao, Y., Zhao, F., & Shi, C. (2017). Influence of thermal processing conditions in 3D printing on the crystallinity and mechanical properties of PEEK material. *Journal of Materials Processing Technology*, 248, 1-7.
- [9] Sanei, S. H. R., & Popescu, D. (2020). 3D-printed carbon fiber reinforced polymer composites: a systematic review. *Journal of Composites Science*, 4(3), 98.
- [10] Roboze. Argo500 Technical Datasheet, <https://www.roboze.com/it/stampanti-3d/argo-500.html> (accessed 13 July 2022).
- [11] Solvay. Ketaspire® CF10 LS1 AM Filament Technical Datasheet, 2019.
- [12] Roboze. Ketaspire® CARBON PEEK Filament Technical Datasheet, 2019.
- [13] ASTM D3039/D3039M-08. Standard Test Method for Tensile Properties of Polymer Matrix Composite Materials.
- [14] Ding S, Zou B, Wang P, et al. Effects of nozzle temperature and building orientation on mechanical properties and microstructure of PEEK and PEI printed by 3D-FDM, *Polym. Test*. 2019, 45: 105948.